OPEN

Experimental & Molecular Medicine (2016) 48, e250; doi:10.1038/emm.2016.61

www.nature.com/emm

ORIGINAL ARTICLE

The p90 ribosomal S6 kinase 2 specifically affects mitotic progression by regulating the basal level, distribution and stability of mitotic spindles

Yun Yeon Park[1,2,3], Hyun-Ja Nam[1,4], Mihyang Do[1,2,3] and Jae-Ho Lee[1,2,3]

RSK2, also known as RPS6KA3 (ribosomal protein S6 kinase, 90 kDa, polypeptide 3), is a downstream kinase of the mitogen-activated protein kinase (MAPK) pathway, which is important in regulating survival, transcription, growth and proliferation. However, its biological role in mitotic progression is not well understood. In this study, we examined the potential involvement of RSK2 in the regulation of mitotic progression. Interestingly, depletion of RSK2, but not RSK1, caused the accumulation of mitotic cells. Time-lapse analysis revealed that mitotic duration, particularly the duration for metaphase-to-anaphase transition was prolonged in RSK2-depleted cells, suggesting activation of spindle assembly checkpoint (SAC). Indeed, more BubR1 (Bub1-related kinase) was present on metaphase plate kinetochores in RSK2-depleted cells, and depletion of BubR1 abolished the mitotic accumulation caused by RSK2 depletion, confirming BubR1-dependent SAC activation. Along with the shortening of inter-kinetochore distance, these data suggested that weakening of the tension across sister kinetochores by RSK2 depletion led to the activation of SAC. To test this, we analyzed the RSK2 effects on the stability of kinetochore–microtubule interactions, and found that RSK2-depleted cells formed less kinetochore–microtubule fibers. Moreover, RSK2 depletion resulted in the decrease of basal level of microtubule as well as an irregular distribution of mitotic spindles, which might lead to observed several mitotic progression defects such as increase in unaligned chromosomes, defects in chromosome congression and a decrease in pole-to-pole distance in these cells. Taken together, our data reveal that RSK2 affects mitotic progression by regulating the distribution, basal level and the stability of mitotic spindles.
Experimental & Molecular Medicine (2016) **48,** e250; doi:10.1038/emm.2016.61; published online 5 August 2016

INTRODUCTION

The Ras/mitogen-activated protein kinase (MAPK) signaling pathway modulates diverse cellular processes, including cell proliferation, survival, growth and migration.[1] Various extracellular growth factors, hormones and cytokines stimulate the Ras–MAPK signaling cascade, which consists of the phosphorylation and activation of the downstream molecules Raf, MEK (MAPK/ERK kinase) and ERK (extracellular signal-regulated kinase).[2] The p90 ribosomal S6 kinase (RSK) family of proteins are also major effectors in the Ras/MAPK signaling pathway downstream of ERK activation.[3] RSKs are characterized by the presence of two functional domains, an N-terminal kinase domain and a C-terminal kinase domain, that are connected by a linker region[3]. Because RSK resides and functions in different subcellular compartments, including the cytosol, the plasma membrane and the nucleus, it is capable of regulating various substrates throughout the cell and affecting a number of biological processes.

To date, four members of the RSK family have been identified in humans. Among them, messenger RNAs for RSK1–3 are known to be expressed ubiquitously in all human tissues, and are regarded as functionally redundant, at least in certain respects.[3] The fact that all six phosphorylation sites known to be associated with the activation of RSKs are highly conserved in RSK1–4 strengthens this viewpoint.[4] However, aberrant activation of each RSK isoform is associated with different human diseases: RSK1 and RSK2 are elevated in breast and prostate cancers;[5] RSK2 activation contributes to fibroblast growth factor receptor-3-expressing multiple myeloma;[6] RSK3 has a tumor-suppressive role in ovarian cancer;[7] and RSK4 is aberrantly expressed in breast cancer.[8] These observations suggest the existence of isoenzyme-specific functions of RSKs

[1]Department of Biochemistry and Molecular Biology, Ajou University School of Medicine, Suwon, South Korea; [2]Genomic instability Research Center, Ajou University School of Medicine, Suwon, South Korea and [3]Department of Biomedical Sciences, The Graduate School, Ajou University, Suwon, South Korea
[4]Current address: Department of Pediatric and Adolescent Medicine, Mayo Clinic College of Medicine, Rochester, MN 55905, USA.
Correspondence: Professor J.-H. Lee, Department of Biochemistry and Molecular Biology, Ajou University School of Medicine, Wonchon Dong San 5, Suwon 443-721, Korea.
E-mail: jhlee64@ajou.ac.kr
Received 7 March 2016; revised 24 March 2016; accepted 29 March 2016

in the tumorigenesis of different tissues. The idea that each RSK isoform has a specific function is further supported by the discovery that Coffin–Lowry syndrome is only associated with mutations in the human *RSK2* gene.[9]

Studies on the involvement of RSK1 and RSK2 in cell cycle regulation have mainly focused on the G1 phase and G2–M transition. There have been relatively fewer reports regarding the role of RSKs in mitotic progression. In *Xenopus laevis* oocytes, both RSK1 and RSK2 are known to regulate cytostatic factor, which is required for metaphase arrest.[10] Specifically, RSK-mediated phosphorylation of Emi2, an anaphase promoting complex (APC) inhibitor, prevents cytostatic factor degradation, thereby inhibiting APC and maintaining metaphase arrest.[11,12] In addition, RSK1 is known to phosphorylate and activate the mitotic checkpoint serine/threonine kinase Bub1, which mediates APC inhibition *in vitro*, indicating that RSK1-mediated Bub1 activation may be responsible for metaphase II arrest during meiosis.[13] The localization of RSK2 at kinetochores under active checkpoint conditions has also been observed.[14] These reports suggest the association of RSKs and spindle assembly checkpoint (SAC) activity in the Xenopus system. In addition, components of the MAPK pathway, including RSK1 and ERK, are localized on mitotic spindles in Swiss 3T3 cells,[15] expanding the mitotic roles of RSKs in mammalian cells. In HeLa cells, RSK2 depletion reduces the kinetochore recruitment of SAC proteins, including Mad1, Mad2 and CENP-E, under active checkpoint conditions.[14] These reports suggest that RSKs might be involved in mitotic progression and/or SAC activation in both Xenopus and mammalian cells; however, their detailed roles throughout mitosis and the mechanisms involved in mammalian cells are not fully understood.

In this study, we show that specific depletion of the RSK2 isoform prolongs the duration of mitosis in association with various mitotic defects, including an increase in misaligned chromosomes and chromosome congression defects. This abnormal mitotic progression caused by RSK2 depletion is accompanied by a reduction in mitotic spindle stability and an irregular distribution of microtubules, indicating the involvement of RSK2 in the regulation of mitotic spindles. Furthermore, the inter-kinetochore distance is shortened in RSK2 knockdown cells in association with increased kinetochore localization of BubR1 (Bub1-related kinase), consistent with a lack of tension between sister chromatids. BubR1 knockdown abrogates the prolongation of mitosis induced by RSK2 depletion. Taken together, these results provide insight into a novel function of RSK2 in controlling the basal level, stability and distribution of mitotic spindles, which in turn affects BubR1-dependent SAC activity.

MATERIALS AND METHODS

Antibodies, chemicals and plasmids

The following antibodies were used: mouse monoclonal antibodies to α-tubulin (Santa Cruz, Dallas, TX, USA, sc-23948), RSK2 (Santa Cruz, sc-9986), BubR1 (BD Transduction, San Jose, CA, USA, 612503) and cyclinB (Santa Cruz, sc-245), and rabbit polyclonal antibody to actin (Sigma, St Louis, MO, USA, A2066), p-p90RSK(Ser380) (Cell Signaling, Danvers, MA, USA, 11989) and p-GSK3β (Santa Cruz, sc-81496) and human anticentromere antibody (ACA; ImmunoVision, Springdale, AR, USA, HRN-0101). All used horseradish peroxidase-conjugated antibodies were obtained from Santa Cruz. The following fluorochrome-conjugated secondary antibodies were used: anti-mouse Alexa-488 (Invitrogen, Waltham, MA, USA, A11059) and anti-human Texas Red (Vector Laboratories, Burlingame, CA, USA, TI-3000). BI-1870 RSK-specific inhibitor was generously provided by Dr. Hilary McLauchlan (University of Dundee, Scotland, UK). MG132 and thymidine were purchased from Sigma-Aldrich. pKH3, HA-tagged WT-RSK2 and HA-tagged RSK2 K/R mutant were generously provided by Dr. John Blenis (Harvard University, Boston, MA, USA).

Cell culture and synchronization by double-thymidine block

HeLa cells were cultured in Dulbecco's modified Eagle's medium nutrient mixture F-12 HAM (DMEM/F-12; Sigma-Aldrich, D8900) supplemented with 10% (v/v) fetal bovine serum (Gibco, Waltham, MA, USA, 16000-044) in 37 °C incubator with 5% CO_2 in air. Cells (7×10^4) were seeded onto 60-mm culture plates, cultured in DMEM/F-12 containing 10% fetal bovine serum for 1 day and treated with 1 mM thymidine (Sigma-Aldrich, T9250) for the first synchronization. Twenty hours later, cells were washed with thymidine-free medium (first release) and cultured in complete medium for 8 h. Then, cells were cultured again in thymidine-containing medium for 14 h for the second round of synchronization. After then, cells were washed with phosphate-buffered saline (PBS) and cultured in fresh medium (final release).

Transfection experiments

High-performance liquid chromatography-purified (>97% pure) short interfering RNA (siRNA) oligonucleotides for the RSK1 and RSK2 knockdown were purchased from Ambion (Austin, TX, USA). The sequences of the sense strands of the siRNA oligonucleotides were as follows: RSK1, 5′-GGCAACGCUGAAAGUACGUdTdT-3′and 5′-GCGAUUCACUGUAUAAACUdTdT-3′; RSK2, 5′ GGCCACAC UGAAAGUUCGAdTdT-3′. Another siRSK2 nucleotide, a pool of three target-specific 20–25-nt siRNAs was purchased from Santa Cruz (sc-36441). HeLa cells (7×10^4) were seeded onto 60-mm dishes. Cells were transfected with 100 nmol each of RSK1, RSK2 or control siRNA oligonucleotides using Oligofectamine (Invitrogen, 58303), according to the manufacturer's instructions. For RSK2 rescue experiments, cells were transfected with DNA or siRNA using Lipofectamine 2000 (Invitrogen, 52887), according to the manufacturer's instructions.

Time-lapse microscopic analysis

Green fluorescent protein-tagged histone H2B-expressing HeLa cells were seeded onto a six-well plate and transfected with siRNA. Twenty-four hours after transfection, two-channel time-lapse video microscopy was performed using a fully motorized Axiovert 200M microscope (Carl Zeiss, Oberkochen, Germany), equipped with AxiocamHRm. Temperature and CO_2 control was maintained using the Pecon Incubator (Houston, TX, USA), S-M and heating insert M06 controlled by Temp control (Erbach, Germany), 37-2 and CTI-Controller (Erbach, Germany), 3700. Both phase contrast and green fluorescent protein fluorescence images were acquired for 48 h with a lapse time of 5 min using AxioVision 4.3 software (Oberkochen, Germany). For routine and quantitative analyses, images were acquired using a ×20 objective lens (LD Plan-Neofluar ×20/0.4 Corr Ph2, Carl Zeiss).

Immunoblotting

Conventional immunoblotting was performed as previously described[16] using indicated antibodies. In brief, cells were washed in PBS and lysed in lysis solution (20 mM Tris–HCl (pH7.4), 150 mM NaCl, 1% Triton X-100, 0.1% SDS, 1 mM EDTA, 5 mM NaF, 0.5 mM Na_3VO_4, 1 mg ml^{-1} leupeptin, 1 mg ml^{-1} Aprotinin). The lysate protein was resuspended in Laemmli sample buffer and boiled for 5 min. The samples were separated by SDS-polyacrylamide gel electrophoresis and then were transferred to nitrocellulose membrane. After blocking for 1 h at room temperature with blocking solution ([PBS containing 0.05% (V/V) Tween-20 and 5% (w/v) non-fat milk), the membranes were incubated with indicated antibodies at 4 °C. Membranes were then washed three times with PBS containing 0.05% Tween-20 and incubated with horseradish peroxidase-conjugated anti-rabbit or anti-mouse antibody for 1 h at room temperature. Detection was carried out using ECL reagents (Amersham Biosciences, Piscataway, NJ, USA, RPN2106) and by exposing them to an X-ray film.

Mitotic index

Condensed chromosomes in mitotic cells were intensively visualized by staining with aceto-orcein solution in 60% acetic acid (Merck, Darmstadt, Germany). Mitotic index was determined by the percentage of mitotic cells with condensed chromosomes.

Cold-stable assay

After siRNA transfection, mitotic cells were collected and incubated with L-15 media (Invitrogen) on ice for 10 min, and then fixed and stained with ACA and α-tubulin. Intensity of cold-stable microtubule was analyzed in $\geqslant$100 cells transfected with siRNAs. Maximum-intensity projections of confocal stacks were produced, and the intensity was measured using Imaris software (Zurich, Switzerland). Scale bar, 2 μm.

Immunofluorescence analysis

Cells were fixed with 3.7% formaldehyde solution and permeabilized with 0.2% Triton X-100. Fixed cells were preincubated in blocking solution (1% bovine serum albumin in PBS), followed by incubation with primary antibodies for overnight at 4 °C. Cells were then washed three times with shaking and probed with fluorescence-conjugated secondary antibody for 1 h at room temperature. For DNA counterstaining, 4′,6-diamidino-2-phenylindole (Molecular probes, Waltham, MA, USA, D3571) was used. After washing, cells were mounted in the mounting solution and examined by a confocal microscope (LSM-710, Carl Zeiss).

Quantification of fluorescent images

Z-series stacks of images at 0.44-μm intervals through each cell were obtained using a Zeiss LSM-710 confocal microscope. For quantification, all images were acquired at identical settings. Metaphase cells were randomly selected and analyzed for the length and width of the congressed body of chromosomes on metaphase plate, BubR1 kinetochore intensity, the inter-kinetochore distance and the pole-to-pole distance. To measure the kinetochore–microtubule fluorescence intensity, a fixed size box (5-pixel width) was placed on the equatorial region using LSM-510 software (Oberkochen, Germany). Data were represented as the ratio of kinetochore–microtubule intensity to control cell intensity. For kinetochore–microtubule distribution, a fixed size box (10-pixel width) was placed on the equatorial region using Zen 2011 software (Oberkochen, Germany). Statistical analysis was performed using the unpaired Student's *t*-test in Excel (Microsoft, Redmond, WA, USA).

RESULTS

Induction of mitotic accumulation by RSK2 depletion

To examine the effects of RSKs on mitotic progression in human cells, we individually depleted RSK1 or RSK2 in HeLa cells using specific siRNAs. Interestingly, depletion of RSK2, but not RSK1, significantly increased the number of mitotic cells, suggesting that RSK2 depletion might cause a mitotic exit defect (Figure 1a). A similar induction of mitotic cell accumulation was observed using separate siRNAs targeting different sequences of RSK2 (Figure 1b), excluding the potential off-target effects of RSK2 siRNA. Considering that RSK2 is a serine/threonine kinase, we tested whether the kinase activity of RSK2 is involved in this mitotic accumulation. Using a rescue strategy, in which wild-type RSK2 or a kinase-dead mutant (K100A) was added back to RSK2-depleted cells, we found that ectopically expressed wild-type RSK2 rescued the mitotic accumulation induced by RSK2 depletion and kinase-dead mutant (K100A) expression also partially rescued this phenotype (Figure 1c), suggesting the possible involvement of both kinase activity-dependent and -independent pathways. The idea that partial involvement of loss of kinase activity here was strengthened by the observation that treatment with BI-D1870, a small-molecule inhibitor of RSK1 and RSK2 kinase activity, induced a concentration-dependent increase in mitotic cell accumulation (Figure 1d). Taken together, these results suggest that RSK2 depletion specifically induces accumulation of mitotic cells, an effect that partially involves the loss of RSK2 kinase activity.

Prolonged mitotic duration induced by RSK2 depletion

Mitotic accumulation usually indicates a change in mitotic progression. To address this, we monitored the mitotic progression of RSK2 siRNA-transfected HeLa cells after release from double-thymidine block. We first checked the time course of mitotic indices, and found that RSK2-depleted HeLa cells exhibited delays in both mitotic entry and exit, with the latter being more greatly affected (Figure 2a). Consistent with the mitotic index data, western blot analyses of samples collected at different times after release from nocodazole arrest clearly showed delayed degradation of cyclin B after RSK2 depletion, indicating a delay in mitotic exit (Figure 2b). Furthermore, time-lapse analyses of green fluorescent protein-histone H2B-expressing HeLa cells for 48 h after siRNA transfection clearly showed a significantly prolonged mitotic duration—from nuclear envelope breakdown to anaphase onset—in RSK2-depleted cells (76.8 ± 93.7 min). Compared with control siRNA-transfected cells (32.2 ± 12.6 min; Figure 2c). The lengthening of mitotic duration was mainly attributable to delayed mitotic exit (metaphase-to-anaphase transition), but also involved prolongation of early mitosis (mitotic

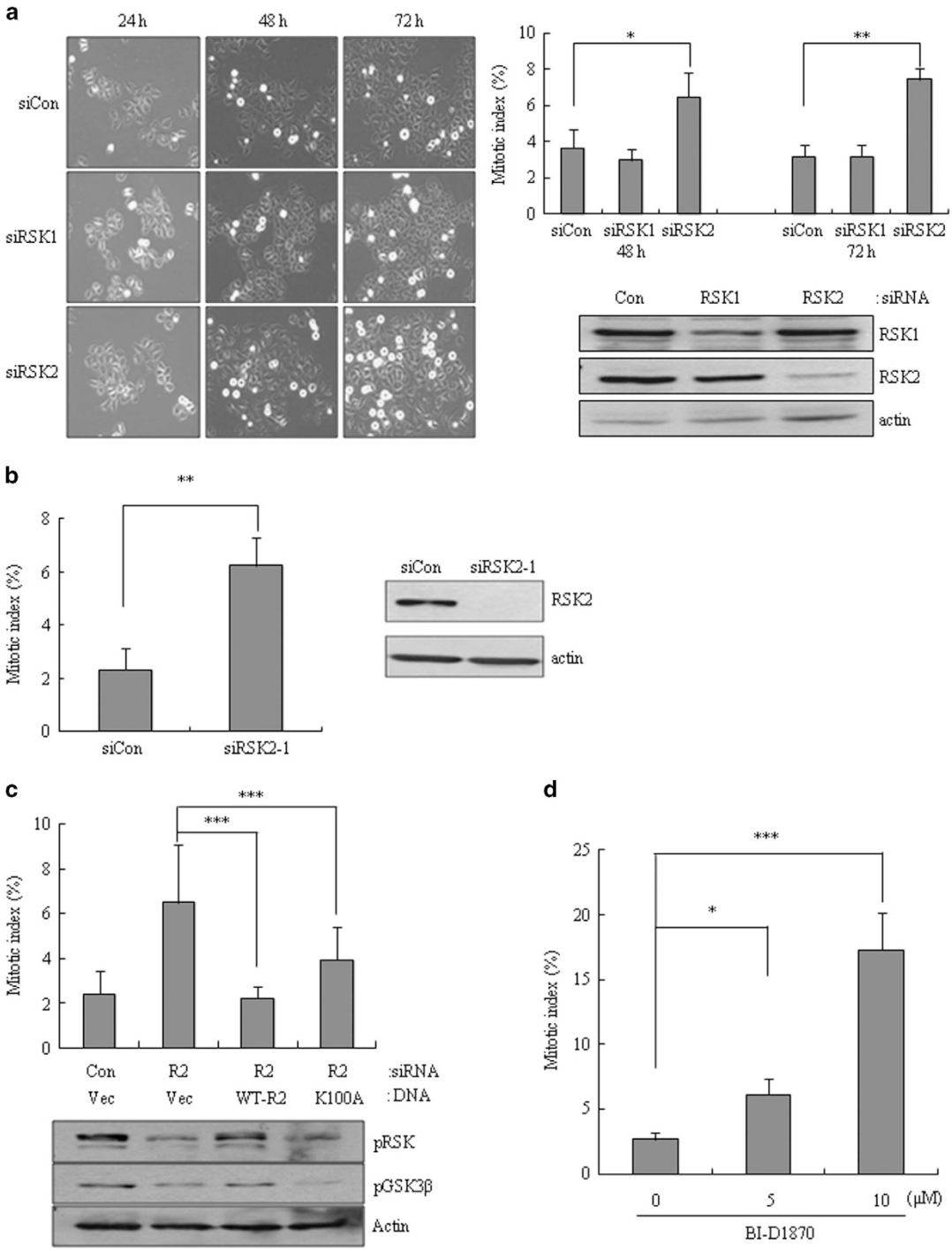

Figure 1 Induction of mitotic accumulation by RSK2 depletion. (**a**) Representative images showing mitotic accumulation at indicated time points after each siRNA transfection (left panel). Cells stained with aceto-orcein were scored for mitosis at indicated time points after each siRNA transfection (right panel, $n=300$). Results are shown as the mean ± s.d. from three independent experiments; $^{*}P<0.05$, $^{**}P<0.01$ by Student's *t*-test. Cell lysates from the indicated samples were subjected to western blot analysis using indicated antibodies. (**b**) Mitotic index was scored after transfection of siRNA targeting different sequences of RSK2 (siRSK2-1; $n=300$). Results are shown as the mean ± s.d. from three independent experiments; $^{**}P<0.01$ by Student's *t*-test. (**c**) Transfection of each RSK2 plasmid DNA into cells was performed 24 h after siRNA transfection. Mitotic cells were scored 48 h after the RSK2 plasmid DNA transfection. (R2, siRSK2; Vec, vector DNA; WT-R2, wild-type RSK2; K100A, kinase-dead RSK2.) Results are shown as the mean ± s.d. from three independent experiments ($n=300$); $^{**}P<0.01$, $^{***}P<0.001$ by Student's *t*-test. (**d**) Mitotic index was, respectively, scored after BI-D1570 treatment. Results are shown as the mean ± s.d. from three independent experiments ($n=300$). $^{*}P<0.05$, $^{***}P<0.001$ by Student's *t*-test. siRNA, short interfering RNA.

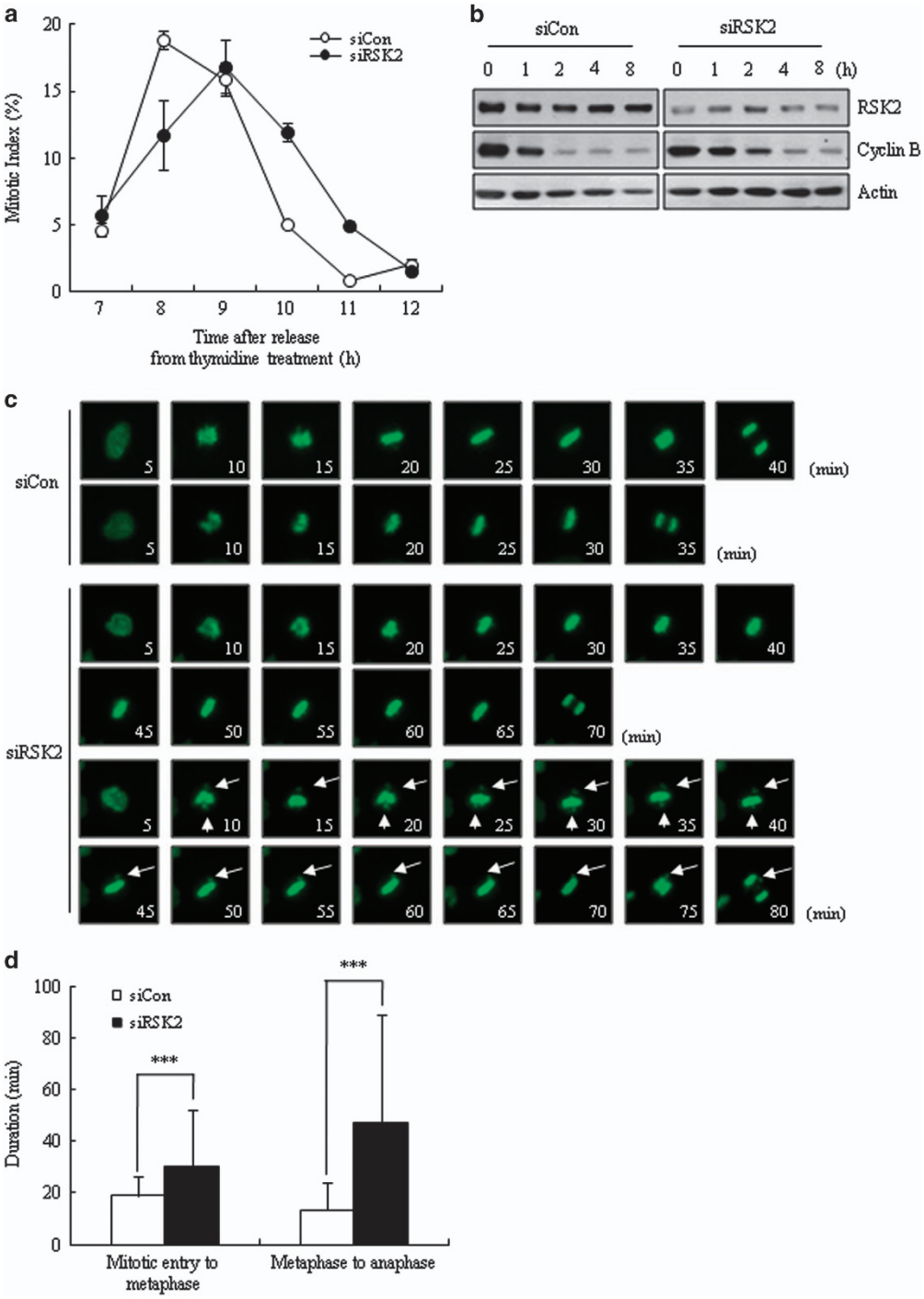

Figure 2 Prolongation of mitotic duration by RSK2 depletion. (**a**) Mitotic index was scored at indicated time points after releasing from thymidine block ($n=300$). A representative data from three independent experiments are shown as mean ± s.d. (**b**) Western blot analysis of cyclin B degradation was performed after releasing from nocodazole treatment (100 ng ml^{-1}) for 16 h. (**c**) Time-lapse microscopy imaging of HeLa cells stably expressing a chromatin marker (H2B–green fluorescent protein; green); rounding up is marked as 0 min. Arrow: unaligned chromosomes. ***$P<0.001$ by Student's *t*-test. (**d**) Mitotic duration was measured from time-lapse images ($n=100$). Mitotic entry time was set as the time of rounding up of the cell. Results are shown as the mean ± s.d. from three independent experiments. ***$P<0.001$ by Student's *t*-test.

entry to metaphase; Figure 2d). Taken together, these results indicate that RSK2 depletion prolongs mitotic duration, affecting metaphase-to-anaphase transition to a greater extent than early mitosis.

Defective chromosome congression and alignment in RSK2-depleted cells

Because the prolongation of mitotic progression implies the existence of defects in mitotic progression, we further

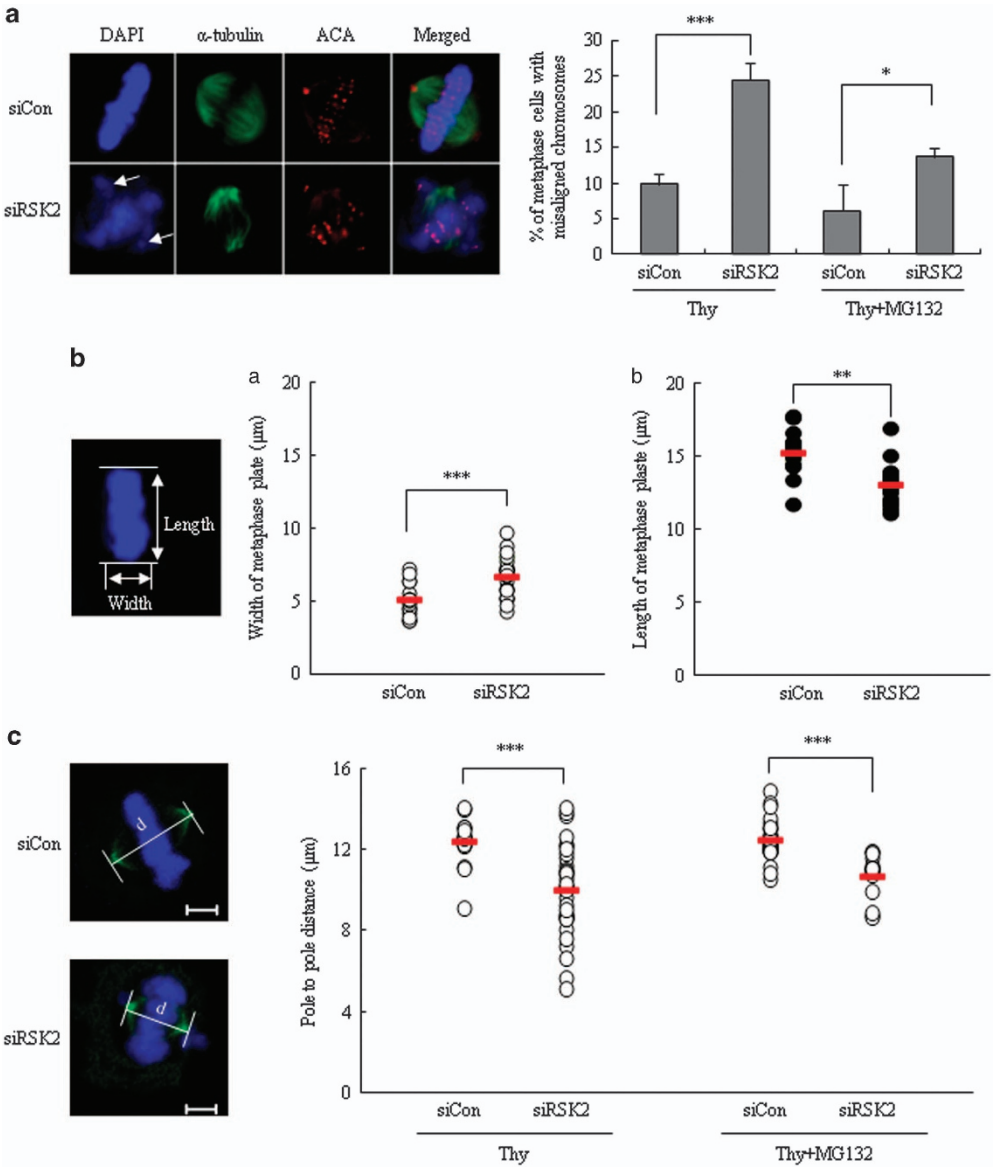

Figure 3 Defects of the chromosome congression and alignment in RSK2-depleted cells. (**a**) Unaligned chromosomes of control and RSK2-depleted cells were measured 8 h after releasing from thymidine block with or without 2 h more incubation with MG132. MG132 was used to give enough time for chromosome congression. Images were representative control (upper left) or RSK2-depleted HeLa cells (lower left) stained for ACA (red), α-tubulin (green) and DNA (blue). Arrow: unaligned chromosomes. Percentage of metaphase cells with unaligned chromosomes. Results are shown as the mean ± s.d. from three independent experiments. $*P<0.05$, $***P<0.001$ by Student's *t*-test ($n=100$). (**b**) The width (a) and length (b) of congressed body of chromosomes on metaphase plate were measured 8 h after releasing from thymidine block. A representative data from three independent experiments are shown as mean ± s.d. $**P<0.005$, $***P<0.001$ by Student's *t*-test ($n=20$). Representative image of metaphase plate was stained with 4′,6-diamidino-2-phenylindole. (**c**) Pole-to-pole distance of metaphase cells (left panel) was measured at 8 h after releasing from thymidine block with or without 2 h more incubation with MG132. A representative data from three independent experiments are shown as mean ± s.d. $***P<0.001$ by Student's *t*-test ($n=16$–36). Representative images of control (upper) or RSK2-depleted HeLa cells (lower) stained for γ-tubulin (green) and DNA (blue). Scale bar, 5 μm.

examined RSK2-depleted cells for the presence of mitotic defects. RSK2-depleted cells exhibited a high incidence of misaligned chromosomes; metaphase cells with misaligned chromosomes accounted for 24.5 ± 2.5% of all mitotic cells in RSK2-depleted cells, but only 9.8 ± 1.5% in control cells (Figure 3a, right panel). Even following treatment with the proteasome inhibitor MG132, which prevents exit from mitosis and thus should provide sufficient time for misalignments to be corrected, the percentage of misaligned chromosomes in RSK2-depleted cells remained high (Figure 3a, right panel). In addition to the increase in misaligned chromosomes at metaphase, RSK2-depleted cells also showed abnormal chromosome congression, as evidenced by an increase in the width of the bodies of aligned chromosomes and a

decrease in their length (Figure 3b). This indicates inefficient chromosome congression during prometaphase, a result consistent with the prolonged duration of the period from mitotic entry to metaphase (Figure 2d). We also measured spindle lengths (pole-to-pole distance) 8 h after release from double-thymidine block. RSK2-depleted cells showed a significant decrease in pole-to-pole distance, suggesting a possible lack of the necessary pushing force against each spindle pole by inter-polar spindles, which might lead to incomplete chromosome congression (Figure 3c). Taken together, these results indicate that depletion of RSK2 induces incomplete chromosome congression as well as an increase in misaligned chromosomes, possibly through the effects on the mitotic spindle that also resulted in decrease of pole-to-pole distance.

Involvement of BubR1 in RSK2 depletion induced accumulation of mitotic cells

Mitotic exit is primarily controlled by SAC activity, which prevents the onset of anaphase and is activated by either unattached kinetochores or a tension defect[17–20]. As prolongation of the mitotic period in RSK2-depleted cells mainly stemmed from a delayed metaphase–anaphase transition (Figure 2d), we assumed that SAC was activated in RSK2-depleted cells. Indeed, immunostaining revealed that the levels of BubR1, a major component of SAC, were significantly enhanced in the kinetochores of RSK2-depleted metaphase cells (BubR1/CREST fluorescence intensity ratio, 0.47 ± 0.25) compared with those from siControl-transfected cells (BubR1/CREST fluorescence intensity ratio, 0.35 ± 0.16; Figure 4a). Retention of BubR1 at the kinetochore generally implies activation of SAC.[21] Staining of the spindle checkpoint protein Mad2, another indicator of SAC activation, did not reveal any significant difference between control and RSK2-depleted cells (data not shown).

As activation of SAC accompanied by BubR1 retention generally means SAC activation due to a tension defect,[22] we measured the tension between two kinetochores by measuring the inter-kinetochore distance between two sister chromatids—the shorter the distance, the lesser the tension. Indeed, the average inter-kinetochore distance in RSK2-depleted cells ($1.08 \pm 0.29\,\mu m$) was decreased significantly compared with that in control cells ($1.33 \pm 0.26\,\mu m$; Figure 4b, left panel). Alternatively, the percentage of cells with inter-kinetochore distance shorter than $1.0\,\mu m$ was significantly increased in RSK2-depleted cells (Figure 4b, right panel). These results indicate that silencing RSK2 attenuated tension across the sister kinetochores, resulting in the subsequent induction of BubR1-dependent SAC activation. To demonstrate the involvement of BubR1-dependent SAC activation in the RSK2 depletion-induced delay in metaphase-to-anaphase transition, we tested whether BubR1 depletion abrogated mitotic prolongation induced by RSK2 depletion. Indeed, BubR1 knockdown in RSK2-depleted cells rescued the increase in mitotic cell accumulation induced by RSK2 depletion, restoring it to a level ($5.61 \pm 0.78\%$) that was similar to that in control cells ($3.07 \pm 0.89\%$; Figure 4c). Moreover, a time-lapse analysis revealed that co-depletion of BubR1 successfully rescued the RSK2 depletion-induced prolongation of mitotic duration (34.50 ± 13.4 min in co-depleted cells vs 69.83 ± 66.1 min in RSK2-depleted cells; Figure 4d). These results clearly indicate that RSK2 depletion induces metaphase-to-anaphase transition delay through BubR1-dependent activation of tension-related SAC.

Decrease in mitotic spindle stability and irregular distribution of mitotic spindles

One common denominator that might explain the decrease in inter-kinetochore tension, decrease in inter-polar distance and congression defect is a change in spindle morphology and/or dynamics. To address this possibility, we first examined spindle dynamics by measuring microtubule re-polymerization after release from nocodazole treatment. Time-course measurements of spindle intensity revealed that the rate of re-polymerization was not different between control and RSK2-depleted cells. Interestingly, however, the plateau intensity level measured as microtubule intensity (in arbitrary units) was significantly decreased in RSK2-depleted cells (Figure 5a, left panel). In line with this observation, measurements of basal α-tubulin intensity in metaphase cells revealed that the intensity of mitotic spindles in RSK2-depleted cells (0.81 ± 0.37) was lower than that in control cells (1.00 ± 0.63; Figure 5a, right panel). These results led us to suspect that RSK2 depletion attenuated the kinetochore–microtubule interactions. Kinetochore–microtubule interactions are revealed by cold treatment, which causes most spindle microtubules to disassemble, whereas allowing kinetochore–microtubules to remain stable. The relative intensity of cold-stable microtubules decreased in RSK2-depleted cells comparing with that of control cells (1.00 ± 0.59 for control cells vs 0.77 ± 0.48 for RSK2-depleted cells; Figure 5b), indicating that kinetochore–microtubules are relatively unstable in RSK2-depleted cells. In human cells, a single kinetochore typically binds 10–30 microtubules.[23] Therefore, a decrease in basal spindle intensity together with diminished kinetochore–microtubule stability would decrease the number of microtubules attached to a single kinetochore, thus reducing inter-kinetochore tension and thereby leading to the activation of BubR1-dependent SAC.

A line-scan analysis of microtubule intensity using *Z*-stack images that show both spindle poles in the same layer revealed an irregular distribution of mitotic spindles along the metaphase plate in RSK2-depleted cells (Figure 5c). The line-scan profile showed that mitotic spindles were relatively scarce in the central region of metaphase plate in RSK2-depleted cells compared with control cells (Figure 5c, left panel). When the length of the metaphase plate was divided into three segments and the intensity of microtubules in the middle segment was compared, microtubule intensity was significantly lower in RSK2-depleted cells than in control cells (Figure 5d), demonstrating the scarcity of microtubules in the central region of the metaphase plate. Microtubules in that area

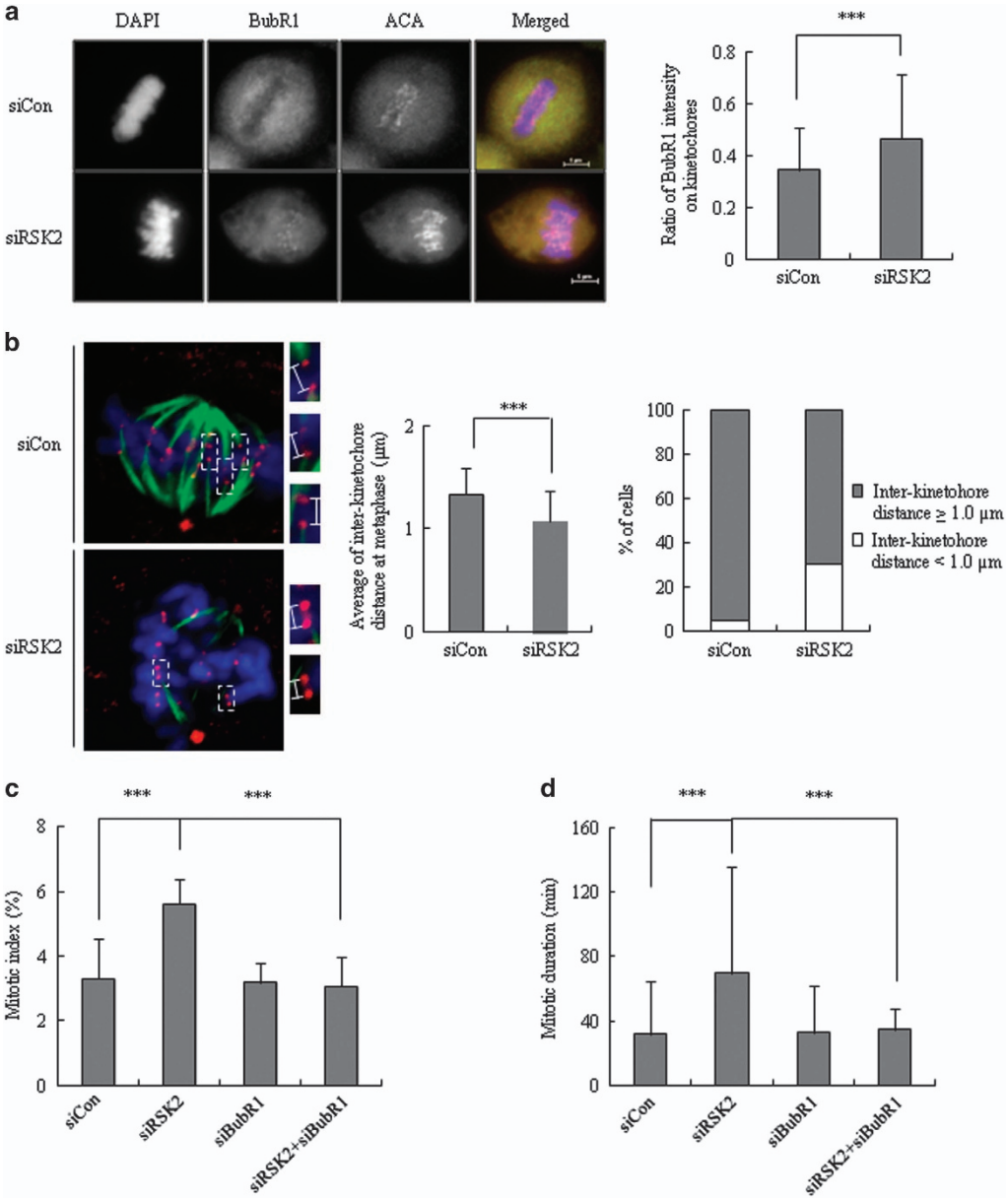

Figure 4 Involvement of BubR1 in RSK2 depletion induced accumulation of mitotic cells. (**a**) Metaphase cells stained for ACA, BubR1 and DNA. Ratio of intensity of BubR1 on kinetochores (ACA) was measured from 80 kinetochore pairs per cell. A representative data from three independent experiments are shown. mean ± s.d. ***$P<0.001$ by Student's *t*-test ($n=10$). Scale bar, 5 μm. (**b**) Inter-kinetochore distance of metaphase cells was measured from >100 kinetochore pairs per cell. Left: a representative data from three independent experiments are shown as mean ± s.d. ***$P<0.001$ by Student's *t*-test ($n=70$). Right: the percentage of the cells having indicated inter-kinetochore distance is shown. A representative data from three independent experiments. (**c**) Mitotic index was measured at 48 h after the transfection with siRSK2 and/or siBubR1. A representative data from three independent experiments are shown as mean ± s.d. ***$P<0.001$ by Student's *t*-test ($n=300$). (**d**) Mitotic duration was measured from the time when cells roundup to anaphase onset. A representative data from three independent experiments are shown as mean ± s.d. ***$P<0.001$ by Student's *t*-test ($n=80$).

probably originate from either kinetochore–microtubules or inter-polar microtubules. As inter-polar microtubules determine pole-to-pole distance,[24] these observations are consistent with the decrease in pole-to-pole distance in RSK2-depleted cells. It is of note that RSK2-depleted cells showed shortened metaphase plate, which may also reflect the changes in the amount and distribution of microtubules in those cells (Figure 3c). Taken together, our findings indicate that RSK2 is involved in maintaining not only microtubule intensity and stability but also a regular distribution of microtubules, which is a prerequisite for uneventful mitotic progression.

DISCUSSION

In this study, we suggest a novel role for RSK2 during mitosis, providing evidence that it regulates the stability and distribution of kinetochore–microtubules, and possibly the inter-polar

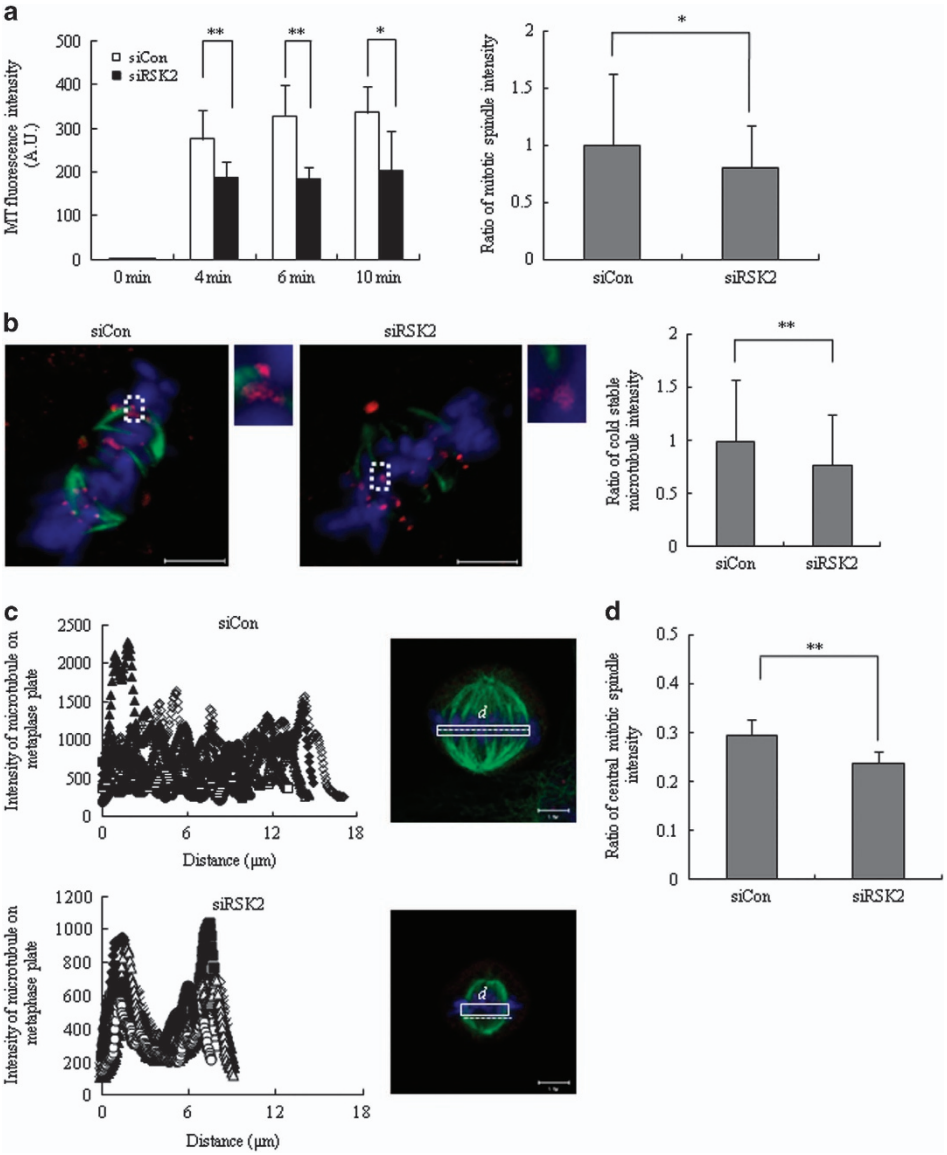

Figure 5 Decrease in mitotic spindle stability and irregular distribution of mitotic spindles. (**a**) The rate of microtubule polymerization was quantified by measuring α-tubulin fluorescence intensity at indicated time points after releasing from nocodazole arrest. A representative data from three independent experiments are shown as mean ± s.d. $*P<0.05$,$**P<0.005$ by Student's *t*-test ($n=8$; left panel). The basal level of spindle intensity from MG132-arrested metaphase cells was measured. A representative data from three independent experiments are shown as mean ± s.d. $*P<0.05$ by Student's *t*-test ($n=80$; right panel). (**b**) After cold treatment for 10 min, remained microtubules on kinetochores were observed (left panel) and its intensity was measured (right panel). Insets in the left panel show enlarged view (indicated by the boxed regions) of optical sections showing individual kinetochore. A representative data from three independent experiments are shown as mean ± s.d. $**P<0.005$ by Student's *t*-test ($n=124$). Scale bar, 5 μm. (**c**) The line-scan profiles of microtubules attached to chromosomes on metaphase plate were visualized, and the intensity of mitotic spindles was measured in white box. $**P<0.005$ by Student's *t*-test ($n=8$). Scale bar, 5 μm. (**d**) The scarcity of microtubule intensity in the central region of metaphase plate. The length of white box in **c** was divided into three. Microtubule intensity in central one-third was measured, and divided by the microtubule intensity of entire white box. $**P<0.005$ by Student's *t*-test ($n=8$).

microtubules, and that its depletion causes several mitotic phenotypes that imply a lack of tension between kinetochore pairs. Although we did not observe any differences in Mad2 localization on unattached chromosomes between control and RSK2-depleted cells (data not shown), BubR1 recruitment to kinetochores was increased in RSK2-depleted cells, and inter-kinetochore distance was decreased. Whether BubR1 is involved in tension-mediated SAC activation has been a matter of controversy. However, the addition of Taxol or low-dose vinblastine to stop kinetochore–microtubule dynamics and reduce tension increases the concentration of BubR1 on kinetochores. Under these conditions, BubR1 and Bub1 are recruited to the kinetochores, whereas Mad2 is not.[20,25,26] Therefore, the prolongation of mitotic duration in RSK2-

depleted cells is highly probably due to tension-dependent SAC activation. Our observation that BubR1 knockdown abrogated the increase in mitotic duration induced by RSK2 depletion (Figure 4c) strongly supports this idea.

Although a few studies have examined the relationship between RSK2 and microtubules during mitosis, RSK2 localization was not consistent from report to report. In our hand, we observed RSK1 localization on mitotic spindles, not RSK2 (data not shown), suggesting that RSK2 is not directly involved in regulating mitotic spindles. Thus, RSK2 seems to act on mitotic spindles indirectly through its yet unidentified substrates. Regarding a candidate substrate protein, it has been reported that phosphorylation of Ran-binding protein-3 by both RSK and AKT/PKB contributes to the formation of a Ran gradient, which is known to be indispensable for kinetochore function, spindle assembly and microtubule dynamics.[27] In addition, we propose that the decrease in microtubule stability and distribution caused by RSK2 depletion may be associated with changes in CENP-S, one of the centromere proteins. Changes in gene expression caused by RSK2 depletion, demonstrated by our microarray screens, included a time-dependent decrease in the messenger RNA level of CENP-S (data not shown), suggesting the possibility that RSK2 depletion reduces the expression of CENP-S and affects the length of the kinetochore outer plate that regulates kinetochore–microtubule stability and distribution. Consistent with this, it has been reported that the depletion of CENP-S induces a mitotic delay similar to that caused by RSK2 depletion and reduces the size of the kinetochore outer plate, thereby contributing to reduced localization of outer kinetochore proteins.[28]

Although the functions of RSKs frequently overlap, individual members of the RSK family also exhibit responsiveness to specific substrate proteins. Previously, we reported that RSK1 functions as a regulator of cytokinesis progression. Depletion of RSK1 caused polyploidy through aberrant localization of the contractile ring components, RhoA and anillin, and abnormal formation of the mid-zone and astral spindles.[16] On the other hand, RSK2 affected SAC activation by regulating the distribution and stability of mitotic spindles rather than cytokinesis progression. According to a list of 36 substrate proteins of RSKs from Blenis group,[29] RSK1 and RSK2 share ~50% of their substrates in common, whereas 50% RSK1 specific and 55% RSK2 specific. Taken together, our findings indicate that the functions of RSK1 and RSK2 differ from each other, even during mitosis, supporting the isoenzyme-specific functions of the RSK family.

In the current study, we demonstrated that the depletion of RSK2 altered the stability and distribution of mitotic spindles. Consistent with this idea, we also observed that constitutive activation of RSK2 enhances kinetochore–microtubule stability and produces lagging chromosomes, chromosome bridges and micronuclei—phenotypes of chromosomal instability that have been reported to result from hyperstable kinetochore–microtubules (unpublished observations). Therefore, these findings support a novel RSK2-specific role: a regulator of mitotic spindles. In conclusion, depletion of RSK2, but not RSK1, induced lengthening of mitotic duration due to the activation of BubR1-dependent tension-sensitive SAC. The decrease in spindle intensity, particularly that of kinetochore–microtubule seems to be the underlying mechanisms. In addition, RSK2 depletion induced abnormal distribution of spindles, particularly sparse spindles at mid-1/3 of the metaphase plate, suggesting the inadequate presence of inter-polar spindles. Collectively, our data suggest that RSK2 influences the basal level, stability as well as distribution of mitotic spindles, thereby guarantees normal mitotic progression.

CONFLICT OF INTEREST

The authors declare no conflict of interest.

ACKNOWLEDGEMENTS

We wish to thank Dr John Blenis (Harvard University, Boston, MA, USA) for providing RSK2 wild-type and kinase-dead mutant constructs. This work was partly supported by the National Research Foundation of Korea (NRF) grant funded by the Korea government (MSIP; no. 2011-0030043), and also supported by the Basic Science Research Program through the NRF funded by the Ministry of Education, Science and Technology (NRF-2012-R1A1A2008333).

1 Roberts PJ, Der CJ. Targeting the Raf-MEK-ERK mitogen-activated protein kinase cascade for the treatment of cancer. *Oncogene* 2007; **26**: 3291–3310.
2 Chen RH, Sarnecki C, Blenis J. Nuclear localization and regulation of erk- and rsk-encoded protein kinases. *Mol Cell Biol* 1992; **12**: 915–927.
3 Fisher TL, Blenis J. Evidence for two catalytically active kinase domains in pp90rsk. *Mol Cell Biol* 1996; **16**: 1212–1219.
4 Dalby KN, Morrice N, Caudwell FB, Avruch J, Cohen P. Identification of regulatory phosphorylation sites in mitogen-activated protein kinase (MAPK)-activated protein kinase-1a/p90rsk that are inducible by MAPK. *J Biol Chem* 1998; **273**: 1496–1505.
5 Schuck S, Soloaga A, Schratt G, Arthur JS, Nordheim A. The kinase MSK1 is required for induction of c-fos by lysophosphatidic acid in mouse embryonic stem cells. *BMC Mol Biol* 2003; **4**: 6.
6 Kang S, Dong S, Gu TL, Guo A, Cohen MS, Lonial S *et al.* FGFR3 activates RSK2 to mediate hematopoietic transformation through tyrosine phosphorylation of RSK2 and activation of the MEK/ERK pathway. *Cancer Cell* 2007; **12**: 201–214.
7 Bignone PA, Lee KY, Liu Y, Emilion G, Finch J, Soosay AE *et al.* RPS6KA2, a putative tumour suppressor gene at 6q27 in sporadic epithelial ovarian cancer. *Oncogene* 2007; **26**: 683–700.
8 Thakur A, Rahman KW, Wu J, Bollig A, Biliran H, Lin X *et al.* Aberrant expression of X-linked genes RbAp46, Rsk4, and Cldn2 in breast cancer. *Mol Cancer Res* 2007; **5**: 171–181.
9 Trivier E, De Cesare D, Jacquot S, Pannetier S, Zackai E, Young I *et al.* Mutations in the kinase Rsk-2 associated with Coffin-Lowry syndrome. *Nature* 1996; **384**: 567–570.
10 Bhatt RR, Ferrell JE Jr. The protein kinase p90 rsk as an essential mediator of cytostatic factor activity. *Science* 1999; **286**: 1362–1365.
11 Inoue D, Ohe M, Kanemori Y, Nobui T, Sagata N. A direct link of the Mos-MAPK pathway to Erp1/Emi2 in meiotic arrest of Xenopus laevis eggs. *Nature* 2007; **446**: 1100–1104.
12 Nishiyama T, Ohsumi K, Kishimoto T. Phosphorylation of Erp1 by p90rsk is required for cytostatic factor arrest in Xenopus laevis eggs. *Nature* 2007; **446**: 1096–1099.
13 Schwab MS, Roberts BT, Gross SD, Tunquist BJ, Taieb FE, Lewellyn AL *et al.* Bub1 is activated by the protein kinase p90(Rsk) during Xenopus oocyte maturation. *Curr Biol* 2001; **11**: 141–150.
14 Vigneron S, Brioudes E, Burgess A, Labbe JC, Lorca T, Castro A. RSK2 is a kinetochore-associated protein that participates in the spindle assembly checkpoint. *Oncogene* 2010; **29**: 3566–3574.

15 Willard FS, Crouch MF. MEK, ERK, and p90RSK are present on mitotic tubulin in Swiss 3T3 cells: a role for the MAP kinase pathway in regulating mitotic exit. *Cell Signal* 2001; **13**: 653–664.
16 Nam H-J, Lee IJ, Jang S, Bae C-D, Kwak S-J, Lee J-H. p90 ribosomal S6 kinase 1 (RSK1) isoenzyme specifically regulates cytokinesis progression. *Cell Signal* 2014; **26**: 208–219.
17 Chen RH, Waters JC, Salmon ED, Murray AW. Association of spindle assembly checkpoint component XMAD2 with unattached kinetochores. *Science* 1996; **274**: 242–246.
18 Nicklas RB, Ward SC, Gorbsky GJ. Kinetochore chemistry is sensitive to tension and may link mitotic forces to a cell cycle checkpoint. *J Cell Biol* 1995; **130**: 929–939.
19 Waters JC, Chen RH, Murray AW, Salmon ED. Localization of Mad2 to kinetochores depends on microtubule attachment, not tension. *J Cell Biol* 1998; **141**: 1181–1191.
20 Nicklas RB. How cells get the right chromosomes. *Science* 1997; **275**: 632–637.
21 Skoufias DA, Andreassen PR, Lacroix FB, Wilson L, Margolis RL. Mammalian mad2 and bub1/bubR1 recognize distinct spindle-attachment and kinetochore-tension checkpoints. *Proc Natl Acad Sci USA* 2001; **98**: 4492–4497.
22 Mao Y, Abrieu A, Cleveland DW. Activating and silencing the mitotic checkpoint through CENP-E-dependent activation/inactivation of BubR1. *Cell* 2003; **114**: 87–98.
23 McEwen BF, Ding Y, Heagle AB. Relevance of kinetochore size and microtubule-binding capacity for stable chromosome attachment during mitosis in PtK1 cells. *Chromosome Res* 1998; **6**: 123–132.
24 Dumont S, Mitchison TJ. Force and length in the mitotic spindle. *Curr Biol* 2009; **19**: R749–R761.
25 Gorbsky GJ, Ricketts WA. Differential expression of a phosphoepitope at the kinetochores of moving chromosomes. *J Cell Biol* 1993; **122**: 1311–1321.
26 Waters JC, Chen R-H, Murray AW, Salmon E. Localization of Mad2 to kinetochores depends on microtubule attachment, not tension. *J Cell Biol* 1998; **141**: 1181–1191.
27 Yoon S-O, Shin S, Liu Y, Ballif BA, Woo MS, Gygi SP *et al*. Ran-binding protein 3 phosphorylation links the Ras and PI3-kinase pathways to nucleocytoplasmic transport. *Mol Cell* 2008; **29**: 362–375.
28 Amano M, Suzuki A, Hori T, Backer C, Okawa K, Cheeseman IM *et al*. The CENP-S complex is essential for the stable assembly of outer kinetochore structure. *J Cell Biol* 2009; **186**: 173–182.
29 Anjum R, Blenis J. The RSK family of kinases: emerging roles in cellular signalling. *Nat Rev Mol Cell Biol* 2008; **9**: 747–758.